Journal of Materials and Environmental Science
ISSN : 2028-2508
e-ISSN : 2737-890X
CODEN : JMESCN

J. Mater. Environ. Sci., 2026, Volume 17, Issue 6, Page 1022-1034

http://www.jmaterenvironsci.com

Metanil Yellow uptake from aqueous solution onto SnO_2 Nanoparticle; Synthesis, Characterization and Optimization of Operational Parameters

Muhammad A. I.[1*] and Abdulfatah S. M.[2]

[1]*Department of Applied Chemistry, Federal University of Technology Babura, Jigawa State.*
[2]*Department of Pure and Industrial Chemistry, Bayero University, Kano.*

Corresponding Author E-mail: maibrahim.chm@futb.edu.ng

Received *20 April 2026,*
Revised *20 June 2026,*
Accepted *21 June 2026*

Keywords:
- ✓ *Metanil Yellow;*
- ✓ *SnO_2 nanoparticle;*
- ✓ *Operational parameters;*
- ✓ *Characterization;*
- ✓ *Adsorption*

Citation*: Muhammad A. I. and Abdulfatah S. M. (2026) Metanil Yellow uptake from aqueous solution onto SnO_2 nanoparticle; Synthesis, Characterization and Optimization of Operational Parameters, J. Mater. Environ. Sci., 17(6), 1022-1034.*

Abstract

Successful synthesis of SnO_2 nanoparticle was conducted for the removal of metanil yellow from aqueous solution. The nanoparticle was synthesized via co-precipitation method and characterized using FTIR, BET, XRD, SEM and EDX. Operational parameters such as contact time, dosage, initial dye concentration, pH and temperature were optimized. The nanoparticle obtained was granular in shape with 265.625 m^2/g surface area and 7.27 nm crystallite size. The Rapid equilibrium adsorption time of 10 minutes and an optimum dosage of 0.6g was obtained. Adsorption capacity increases with an increase in concentration and decreases with a decrease in pH and temperature. The result showed a remarkable performance of the nanoparticle for the effective uptake of the dye.

1. Introduction

The rising level of water pollution, driven by industrialization and agricultural expansion, is of grave environmental concern (Dutta *et al.*, 2021). Untreated or partially treated aqueous wastewater from various industries is interspersed with mainstream water resources, which is detrimental to human life and aquatic organisms. Dyes are a significant class of recalcitrant toxic water contaminants emanating alongside various pigments and byproducts from many industries (Shaikh *et al.*, 2021; Akartasse *et al.*, 2022). Of the over 11800 commercially available dyes/pigments, the annual global consumption is estimated at around 19 million metric tons. Textile (42.6%), paint and coating (27.8%), plastic (16.3%), and paper, cosmetics and ink (13.3%) industries are the major consumers of dyes (Moosavi *et al.*, 2020). Around 10–15% industrial dyes

are released into the environment during manufacturing and processing operations (Moosavi *et al.*, 2020).

Numerous techniques have been employed to clean dye polluted water (Alkhadra *et al.*, 2022). However, conventional treatment methods are cumbersome, expensive, time and energy-consuming, and exhibit low removal efficiency and residual discharge (Ganguly *et al.*, 2020). Adsorption and photocatalytic degradation of pollutants have caught the attention of many researchers, being simple, environment-friendly alternative, with minimum sludge formation, and high mineralization efficiency (Wen *et al.*, 2019). Over last few decades, a variety of materials have been developed for the adsorptive removal of toxic dyes which include nanogels (Khan *et al.*, 2024; Nangia *et al.*, 2023), metal-oxide nanocomposites (Yaseen *et al.*, 2022; Latifi *et al.*, 2025), metal organic frameworks (Tchinsa *et al.*, 2021), plant-based materials (Manzoor *et al.*, 2024), and activated carbon/biochar (Cheng *et al.*, 2021; Kumar *et al.*, 2023) because of their ease of preparation, inexpensiveness, effectiveness over a wide range of pollutants, and porous structure with high adsorption capabilities and kinetics.

Tin dioxide (SnO_2) nanoparticles are highly effective in wastewater treatment due to their strong adsorption capacity, high surface-to-volume ratio, and excellent photocatalytic properties (Rguiti *et al.*, 2018; Abdulhameed *et al.*, 2025; Muniyappa *et al.*, 2025; Moussa *et al.*, 2025). Tiwari *et al.*, (2025) published interesting research on SnO_2 nanomaterials concerning dye degradation in wastewater treatment. The remarkable photocatalytic activity of SnO_2 led to the removal efficiencies greater than 90% for methylene blue and rhodamine B at optimum conditions of pH, light, and exposure time.

Therefore, the primary objective of this research is to investigate the adsorption of metanil yellow (MY) dye from aqueous solution using SnO_2 nanoparticles. By doing so, this study aims to address the challenges associated with treating dye pollutants and pave the way for more efficient method of water purification.

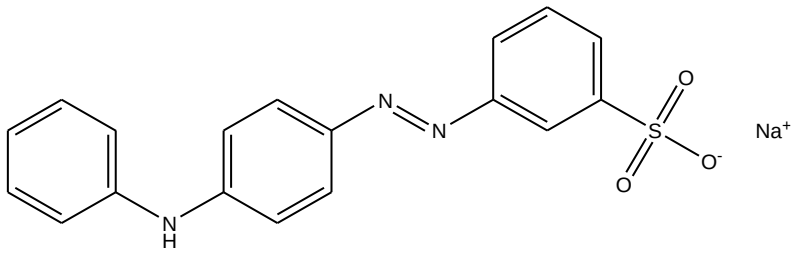

Figure 1: Structure of Metanil yellow dye (Chiou and Chuang, 2004)

2. Materials and methods

2.1 Materials

The instruments/equipment used in this research are Analytical electronic weighing balance (FA 2004), pH (Jenway 3510), Parkin Elmer UV-Visible spectrometer (Labda 35: Perkin Elmer), Fourier transform infrared spectroscopy (Cary 630; Agilent Technologies), Incubator shaker (Innova 4000 incubator shaker), and Scanning Electron Microscope (SEM, Leica Stereoscan-440 interfaced with Phoenix EDX).

The reagents used for the research are Tin (II) chloride dihydrate ($SnCl_2.2H_2O$) (99%), Sodium hydroxide (NaOH) (99%), Sodium chloride (98%), Methanol (99%), Metanil Yellow dye (70% Merck) and Ammonia.

2.2 Methods

2.2.1 Synthesis of Tin Oxide Nanoparticle

In the present work tin oxide (SnO_2) nanoparticles were synthesized by the co-precipitation method using precursor stannous chloride and methanol. 3.5 g of stannous chloride was dissolved in 100 ml of methanol and kept under magnetic stirring for 30 minutes. 10 ml of ammonia (NH_3) was rapidly injected into the container and was continuously stirred for an additional 30 minutes. Following rapid injection, a white precursor was obtained and the reaction system gradually became transparent and the color changes slowly, the color changes from transparent to white. The white colour precipitate was taken out by filtering and then the filtered powder was washed with methanol. The washed nanoparticles were dried at 60 ºC for 4 hours by using hot air oven. The prepared nanoparticles were annealed 200 ºC for 2 hours in hot air oven for characterization (Balakrishnan and Murugesan, 2020).

2.2.2 Characterization

2.2.2.1 Fourier Transform Infrared (FTIR) Spectroscopy

FT-IR measurements of the tin oxide nanoparticles were carried out to identify the possible functional groups that may be responsible for the adsorption of metanil yellow (MY) dye using FTIR Cary 630 from Agilent technologies and the spectra were recorded in the wavelength interval 4000 to 600 cm^{-1}.

2.2.2.2 Scanning Electron Microscopy (SEM)

The Surface morphology of the synthesized SnO_2 nanoparticles was examined using scanning electron microscopy (SEM). SEM analysis was carried out at selected regions of the sample to obtain high-resolution topographic and morphological images with improved depth of focus, following the method reported by Eddy *et al.*, (2014).

2.2.2.3 Brunauer-Emmett-Teller (BET) Analysis

The specific surface area of the prepared SnO_2 nanoparticles was determined using the Brunauer-Emmett-Teller (BET) method. BET analysis was performed based on nitrogen adsorption-desorption isotherms to evaluate the surface area of the samples, following the procedure described by Marwani *et al.*, (2014).

2.2.2.4 X-Ray Diffraction Analysis

X-ray diffraction measurement was carried out to determine the crystal phase composition and size of the nanocomposite. The average crystallite size (D) was calculated from XRD pattern according to the Scherrer equation as shown in **Equation 1**:

$$D = \frac{K\lambda}{\beta COS\phi} \quad (1)$$

where, k is constant (about 0.9), λ is the wavelength (0.15405 nm), β is the full width at half maximum (FWHM) of the diffraction line and θ is the diffraction angle (Habib *et al.*, 2018)

2.2.2.5 Energy Dispersive X-ray Spectroscopy (EDX)

Energy dispersive x-ray spectroscopy (EDX) was used to determine the elemental composition of the synthesized nanomaterials. The analysis was carried out to confirm the surface elemental composition relevant to photocatalytic and adsorption applications following the method reported by (Awfa *et al.*, 2018).

2.2.3 Adsorption studies

Batch Adsorption Experiment

The influence of variables including, amount of adsorbent, contact time, temperature, pH and Initial concentration on the removal of MY was investigated in batch mode at room temperature (30 ± 3 ^{o}C). In each experiment, 100 cm^3 of dyes in a 120 cm^3 bottle was agitated and stirred at 200 rpm along with a fixed mass of the nanoparticles at constant temperature. The final concentration of the dye was determined spectrophotometrically using UV-Visible spectrophotometer (Hitachi 2800) at a predetermined corresponding λ_{max} 431 nm (Ibrahim and Ibrahim, 2018). The equilibrium adsorption capacities of the adsorbates will be calculated using **Equation 2**:

$$q_e = \frac{(C_O - Ce)V}{M} \qquad (2)$$

Where C_0 and C_e are the initial concentration and concentration of the adsorbate at equilibrium, V is the volume of the solution and M is the mass of the adsorbent.

3. Results and discussion

3.1 Fourier Transform Infrared (FTIR) Spectroscopy

FTIR Spectroscopy is often use to detect different functional groups on the surface of the synthesized nanomaterials. Functional group determination is very important in understanding adsorption phenomena. Figure 2 presents the FTIR Spectra of SnO_2, before and after adsorption with MY dye. The absorption peak at 3508cm^{-1} represents the presence of OH stretching vibrations, the C – H stretching were observed at 2883cm^{-1} (Ma *et al.*, 2017). C≡C stretching vibrations were observed at 2108 and 2136 cm^{-1}, and the absorption band observed at 1985 cm^{-1} reflects the skeletal stretching of the allene group. The peaks around 600 – 700 cm^{-1} can be attributed to the Sn – O band (Lv *et al.*, 2006).

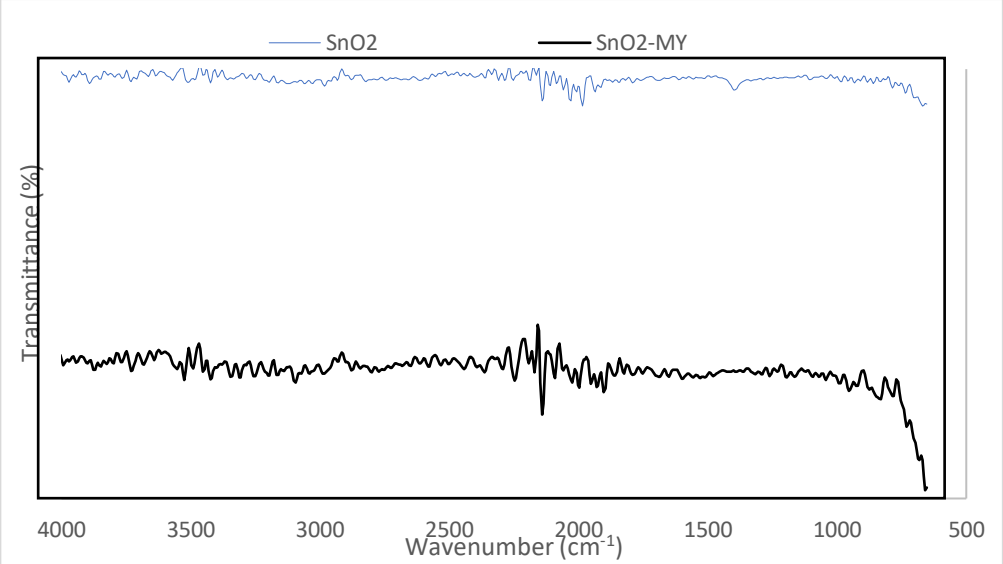

Figure 2: FTIR Spectra of SnO_2 Nanoparticle before and after Adsorption

3.2 Brunauer-Emmett-Teller (BET) Analysis

Brunauer-Emmett-Teller (BET) theory aims to explain the physical adsorption of gas molecules on a solid surface and serves as the basis for an important analysis method for the measurement of the specific surface area of prepared nanomaterials (Marwani *et al.*, 2014). The surface area, pore volume, micro-pore surface area and pore diameter of SnO_2-Np are presented in **Table 1**. SnO_2-Np was found to have 265.625 m^2/g surface area, 0.130 cc/g pore volume, 249.093 m^2/g micro-pore surface area and 2.132 nm pore diameter respectively.

Table 1: Brunauer-Emmett-Teller (BET) Analysis

Adsorbent	Surface Area (m^2/g)	Pore Volume (cc/g)	Micropore Surface Area (m^2/g)	Pore Diameter (nm)
SnO_2	265.625	0.130	249.093	2.132

3.3 X-Ray Diffraction Analysis

Figure 3 represents the XRD patterns of SnO_2-Np. Crystallinity and crystal phases of the synthesized materials were investigated. In the XRD pattern, many peaks are found at the 2θ angles of 16.61º, 27.9º, 37.81º which correspond with Bragg's planes of (110), (101), and (200). The average crystallite size was calculated to be 7.27 nm using Debye Scherer Equation.

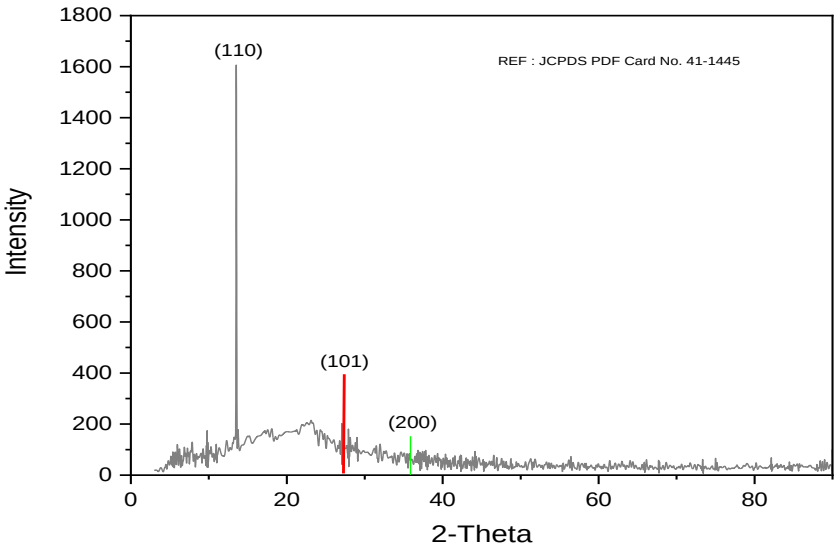

Figure 3: XRD Patterns of SnO_2-Np

3.4 Scanning Electron Microscopy (SEM)

Scanning Electron Microscopy (SEM) involves examining the surface morphology of the adsorbent material before and after adsorption process. It allows us to determine changes in surface morphology, such as the deposition of dye molecules, roughness at the surface which can provide insights into the adsorption mechanism and efficiency of the adsorbent material (Liu *et al.*, 2021). SEM images of SnO_2 nanomaterial show that the nanoparticles are granular in size and have irregular spherical morphology as shown in **Figure 4**. Appreciable changes were observed in the micrographs after the adsorbent have been loaded. The changes are indication that there is interaction between the dye molecule and the adsorbent surface.

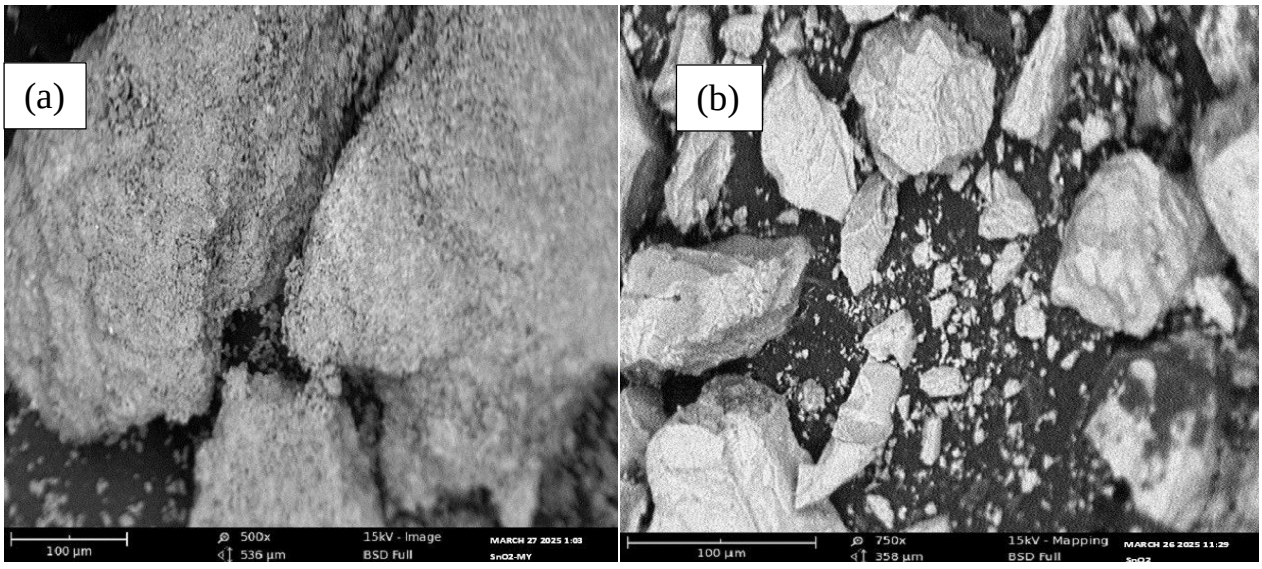

Figure 4: SEM Micrographs of SnO_2-Np a) Before adsorption b) After Adsorption with MY

3.5 Energy Dispersive X-ray Spectroscopy (EDX)

Energy dispersed spectroscopy reveals the elemental composition of the nanomaterials. The EDX spectra of SnO_2-Np with the atomic content of the elements are shown in **Figure 5**. This information is essential, considering adsorption process is dependent on surface chemistry (Awfa *et al.*, 2018).

Element	Atomic %	Weight %
Sn	68.62	67.34
O	21.48	25.85

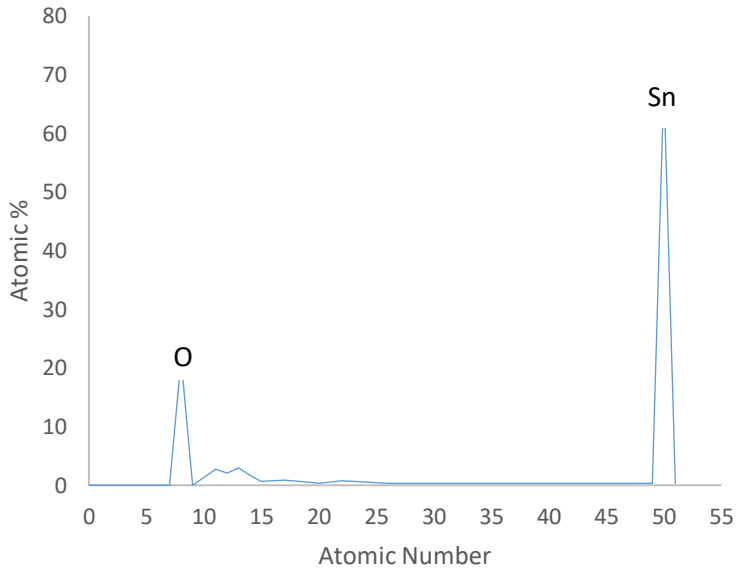

Figure 5: EDX Spectrum of SnO_2 Nanoparticle

The EDX spectra show that all the synthesized nanomaterials are pure with minute impurities. The observed atomic percentages of all the elements are shown in **Figure 5**. The atomic percent of Sn was 68.62% and oxygen was 21.48%, respectively. The presence of some impurities is due to the coating in the imaging process (Singh *et al.*, 2022) and others are in the precursor salt used during the synthesis of the nanomaterials.

3.6 Batch Adsorption Studies

Batch Adsorption experiments were carried out to Study the Effect of Experimental parameters. Effect of experimental Parameters such as Effect of Contact time, adsorbent dosage, Initial dye concentration, pH and Temperature were carried out.

3.6.1 Effect of Contact Time

One of the most foremost factors to fabricate an efficient adsorbent for wastewater treatment is the contact time factor (Gupta and Saleh, 2013; Kumari *et al.*, 2017). **Figure 6** shows the results of influence of contact time on the adsorption of MY dye molecules using SnO_2 which is studied through various time intervals (1–60 min). Other parameters such as pH, concentration, dosage and temperature. The results illustrate a rise in adsorption capacity with increase in contact time between the adsorbent and adsorbate. With increase in agitation time, the external transfer coefficient increases resulting in higher adsorption of the dye molecules. The dye molecules first

encounter the boundary layer effect, then adsorption at the surface and finally diffusion into the porous structure of the Adsorbent (Alabi *et al.*, 2023).

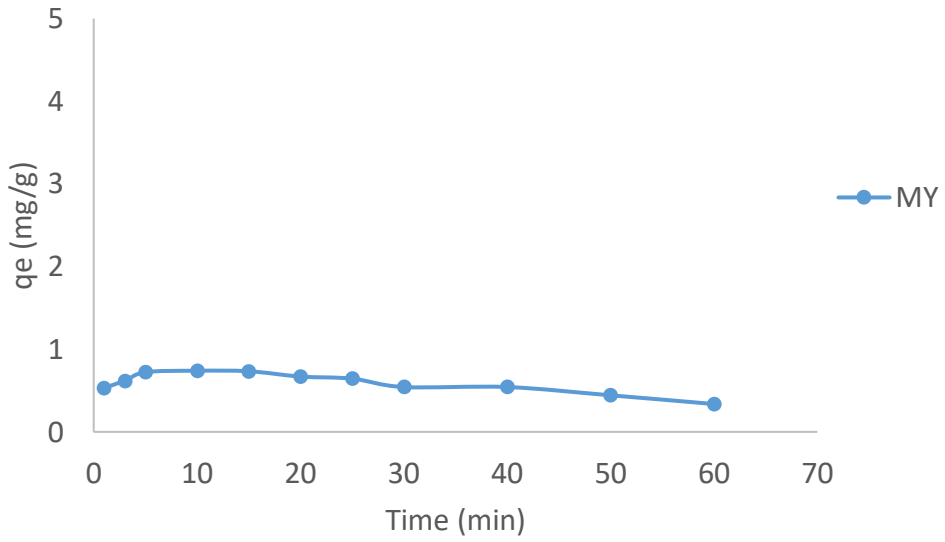

Figure 6: Effect of Contact Time on the Removal of MY & MY + AB Using SnO_2

The equilibrium time obtained is 10 minutes. The rapid uptake at early stage is due to large concentration gradient between the bulk liquid and the solid surface adsorbate concentration. This is attributed to large amount of active sites available for adsorption. The adsorption active sites were then reduced as the adsorption time increase (Moufi *et al.*, 2016), the decrease might be due to exhaustion of active sites and repulsive force between the adsorbent and adsorbate. Similar results showing fast adsorption process were reported by Senapati *et al.* (2025) during ultra-fast adsorption of the industrial cationic dye pollutant using nitric acid-activated rice straw biochar: insights into adsorption mechanisms and Ibrahim and Ibrahim (2018) during Copper (II) Oxide particles as Adsorbent for Removal of Alkali Blue; Isotherm and Kinetic Studies.

3.6.2 Effect of Adsorbent Dosage

The determination of the effect of adsorbent dose is very important because it estimates the capacity of adsorbent to remove the amount of dye. Initially the amount of dye adsorption increases because of empty active sites on the adsorbent surface (Ehrampoush *et al.*, 2011). **Figure 7** shows the results of effect of adsorbent dosage on the adsorption of MY dye molecules using SnO_2 which was studied through various dosage varied from (0.2–1.0 g). Other parameters such as pH, concentration, dosage and temperature. For the adsorption of MY onto SnO_2 there were sharp increase in the adsorption capacity from 0.2 – 0.6 g, from 0.6g there was decrease in the adsorption capacity. The decrease may be due to decrease in the surface area available resulting from overlapping or aggregation of adsorption sites as similarly observed by Nethaji *et al.* (2013).

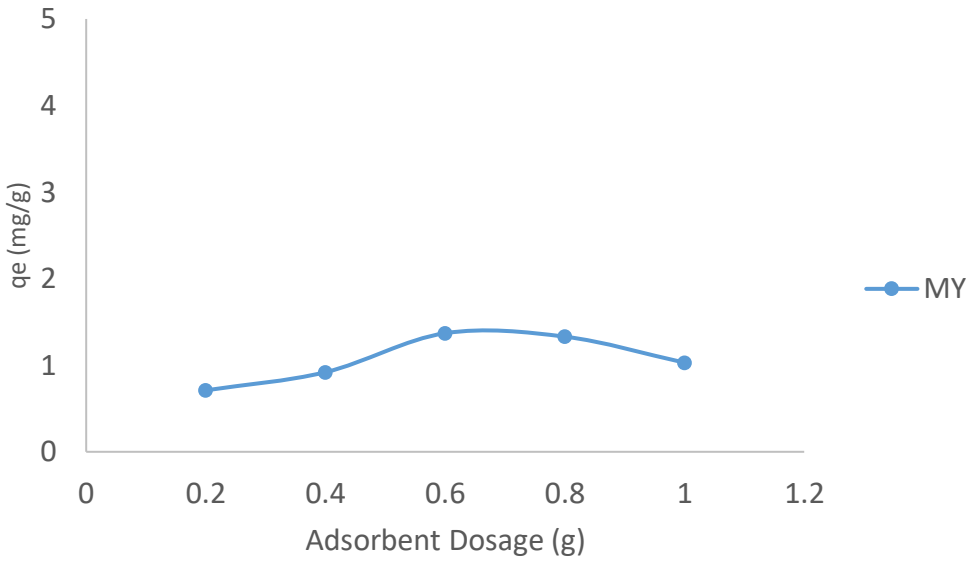

Figure 7: Effect of Dosage on the Removal of MY Using SnO_2

3.6.3 Effect of Initial Dye Concentration

Initial dye concentration is responsible for the mass transfer between aqueous and solid phases because it provides the driving force. Increase in initial dye concentration may increase or decrease the percentage dye removal depending on the nature of dye (i.e., cationic or anionic). The amount of dye (mg/g) removed increases with increases in initial dye concentration (Bazrafshan *et al.*, 2013). **Figure 8** shows the results of effect of Initial dye Concentration on the adsorption of MY dye molecules using SnO_2 in which various concentrations of 10, 20, 30, 40, 50, 100, 150, 200, 250 mg/L was studied. The study revealed that the adsorption capacity of MY increase with increase in initial concentration. The increase in adsorption capacity with increase in concentration can be attributed to the increased driving force and utilization of more of the active sites available for adsorption at higher concentration. Similar trend of increase in adsorption capacity with increase in temperature was reported by Salmani *et al.* (2017) during Modification of pomegranate waste with iron ions a green composite for removal of Pb from aqueous solution: equilibrium, thermodynamic and kinetic studies.

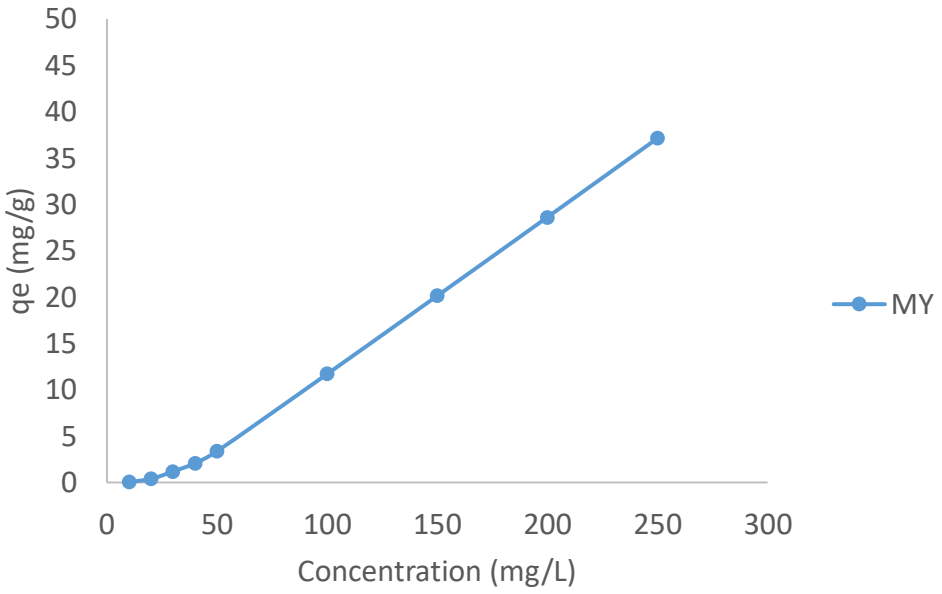

Figure 8: Effect of Concentration on the Removal of MY Using SnO_2

3.6.4 Effect of pH

The solution pH is the main factor affecting the sorption experiments due to its control on the adsorption process by affecting surface charges of the stationary layer of the sorbent surface and dissociation of functional groups of the active sites. Adsorption is largely influenced by surface interactions between adsorbed molecules and sorbent functional groups. These interactions lead to bonding between the adsorbent surface and the adsorbate molecules (Najafi *et al.*, 2022). **Figure 9** shows the results of effect of pH on the adsorption of MY dye molecules using SnO_2. pH of the dyes was varied from 2- 12. The adsorption capacity of MY decreases with increase in pH. MY is an anionic dye that exist in the form of negatively charged ions when in aqueous solution. The rate of adsorption onto the surface of the adsorbent is controlled by the surface charge on the adsorbent which is influenced by the pH of the solution (Alqarni, 2022). High adsorption capacity at lower pH was observed. The acidic medium is favourable for the adsorption of the dye. High adsorption capacity of anionic dyes at low pH indicates that the surface of the adsorbent appear to be acidic which increase the protonation at their surface due to neutralization of negative charges and resulting in easier diffusion. This provides more active surface of the adsorbents and result into more adsorption at their surface. On increasing pH deprotonation takes place which decreases the diffusion and adsorption (El-Dars *et al.*, 2016).

3.6.5 Effect of Temperature

The effect of temperature was studied by varying the temperature from 303 to 333 K. **Figure 10** shows the results of effect of Temperature on the adsorption of MY dye molecules using SnO_2. The results shows that there is decrease in the adsorption capacity MY with increase in temperature on their adsorption onto SnO_2. The decrease in adsorption capacity with increase in temperature is attributed to desorption of weakly bonded or physisorbed adsorbates molecules due to increased solubility in liquid phase. The physisorbed molecules are far from the surface (low binding energy) and require lower energy for desorption. With increase in temperature, the

attractive forces between adsorbent surface and dye molecules are weakened and the adsorption decreases (Ibrahim and Ibrahim, 2018). This suggest that the adsorption of MY onto SnO_2 is controlled by physical forces because for chemical adsorption, an increase in temperature normally enhance the adsorption capacity and the kinetic energy also increases, accelerating the diffusion of adsorbate molecules from the solution to the adsorbent (Kebede *et al.*, 2018).

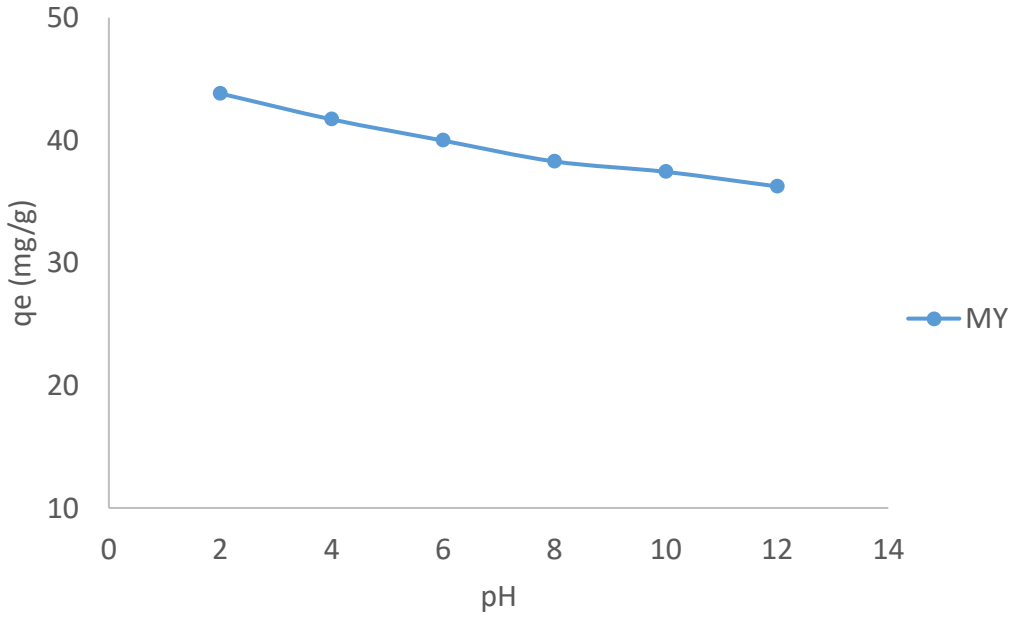

Figure 9: Effect of pH on the Removal of MY Using SnO_2

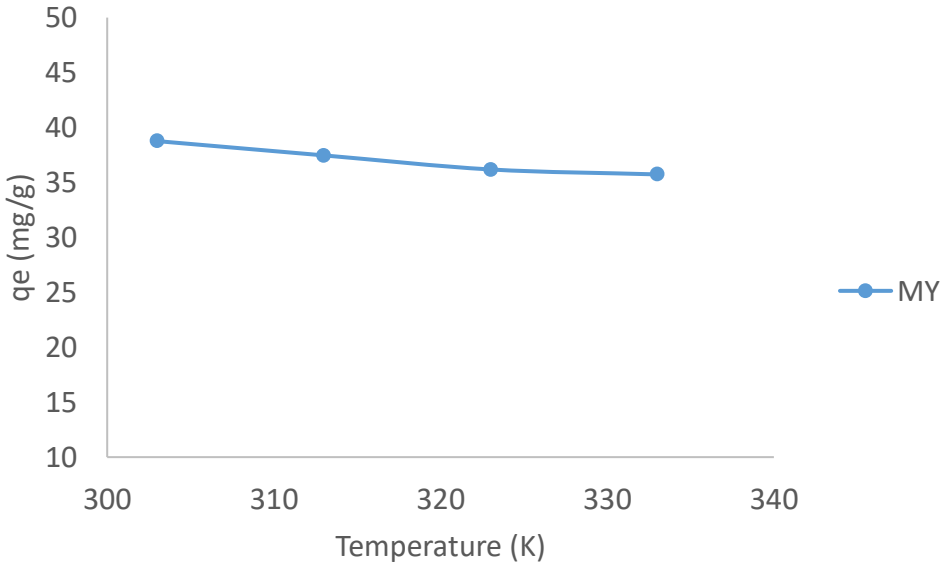

Figure 10: Effect of Temperature on the Removal of MY Using SnO_2

Conclusion

A highly effective nanomaterial was synthesized and utilized for the uptake of metanil yellow dye. The nanoparticle was synthesized using co-precipitation method and characterized using various characterization techniques. Various operational parameters such as time, dosage, concentration,

temperature and pH were optimized. The results revealed a good nanoparticle with high surface area and very small crystallite size. The adsorption process was very rapid, increases with increase in concentration and decreases with increase in temperature and pH. In conclusion, the synthesized nanoparticle showed a positive response toward the removal which will pave way to utilize an effective nanomaterial for water treatment application.

Acknowledgement: Department of Pure and Industrial Chemistry, Bayero University Kano is acknowledged.
Disclosure statement: *Conflict of Interest*: The authors declare that there are no conflicts of interest.
Compliance with Ethical Standards: This article does not contain any studies involving human or animal subjects.

References

Abdulhameed, A. S., Al Omari, R. H., Abdullah, S., Al-Masud, A. A., Abualhaija, M., & Algburi, S. (2025). Nanoarchitectonics of biohybrid polymer nanocomposite of carboxylated chitosan-phthalate/SnO2 nanoparticles for dye wastewater treatment: characterisation, isotherm, kinetic, and adsorption optimisation. *International Journal of Environmental Analytical Chemistry*, 105(18), 6799–6820. https://doi.org/10.1080/03067319.2024.2429792

Akartasse N., Azzaoui K., Mejdoubi E., Hammouti B., Elansari L.L., Abou-salama M., Aaddouz M., Sabbahi R., Rhazi L. and Siaj M. (2022), Environmental-Friendly Adsorbent Composite Based on Hydroxyapatite/Hydroxypropyl Methyl-Cellulose for Removal of Cationic Dyes from an Aqueous Solution, *Polymers*, 14(11), 2147; https://doi.org/10.3390/polym14112147

Alabi, A. H., Hashirudeen, M. M., Olaleye, R. K. and Oladele, E. O. (2023). Adsorption of organic dyes by carbonized and chemically activated *Cassia fistula* pods. *Journal of Materials and Environmental Sustainability Research,* 2(3): 12-36.

Alkhadra, M. A., Su, X., Suss, M. E., Tian, H., Guyes, E. N., Shocron, A. N., Conforti, K. M., De Souza, J. P., Kim, N., Tedesco, M., Khoiruddin, K., Wenten, I. G., Santiago, J. G., Hatton T. A. and Bazant, M. Z. (2022). Electrochemical Methods for Water Purification, Ion Separations, and Energy Conversion, *Chem. Rev.*, 122, 13547–13635.

Alqarni, S. A. (2022). Deliberated system of ternary core-shellpolythiophene/ZnO/MWCNT sandpolythiophene/ZnO/ox-MWCNTs nanocomposites for brilliant green dye removal from aqueous solutions. *Nanocomposites*. 8(1): 47-63

Awfa, D.; Ateia, M.; Fujii, M.; Johnson, M.S.; Yoshimura, C. (2018). Photodegradation of Pharmaceuticals and Personal Care Products in Water Treatment Using Carbonaceous-TiO_2 Composites: *A Critical Review of Recent Literature. Water Res.*, 142, 26–45.

Balakrishnan, K. and Murugesan N. (2020). Synthesis and characterization of SnO2 nanoparticles by co-precipitation method. *Int. J. Nano Dimens.*; 12(1): 76-82.

Bazrafshan, E., Mostafapour, F. K., Hosseini, A. R., Khorshid, A. R. and Mahvi, A.H. (2013). Decolorisation of reactive red 120 dye by using single-walled carbon nanotubes in aqueous solutions. *J. Chem.*, 2013, 938374.

Cheng, L., Ji, Y., Liu, X., Mu L. and Zhu, J. (2021). Sorption mechanism of organic dyes on a novel self-nitrogen doped porous graphite biochar: coupling DFT calculations with experiments, *Chem. Eng. Sci.*, 242, 116739.

Dutta, D., Arya, S. and Kumar, S. (2021). Industrial wastewater treatment: current trends, bottlenecks, and best practices, *Chemosphere*, 285, 131245.

Eddy N. O., Udofia I., Uzairu A., Odiongenyi A.O., and Obadimu C. (2014). Physicochemical, Spectroscopic and Rheological Studies on *Eucalyptus Citriodora (EC)* Gum, *Journal of Polymer and Biopolymer Physics Chemistry*, 2(1), 12-24.

Ehrampoush, M.; Ghanizadeh, G.; and Ghaneian, M. (2011). Equilibrium and kinetics study of reactive red 123 dye removal from aqueous solution by adsorption on eggshell. J. Environ. Health Sci. Eng., 8, 101–106.

El-Dars, E. M. S., Ibrahim, H. M., Farag, H. A. B., Abdelwahhab, M. Z. and Shalabi, M. E. H. (2016). Preparation and Characterization of Bentonite Carbon Composite and Design Application in Adsorption of Bromothymol Blue Dye. *Journal of Multidisciplinary Engineering Science and Technology.* 3(1) 3758-3765.

Ganguly, P., Sarkhel, R. and Das, P. (2020). Synthesis of pyrolyzed biochar and its application for dye removal: batch, kinetic and isotherm with linear and non-linear mathematical analysis, *Surf. Interfaces*, 20, 100616.

Gupta, V. K., and Saleh, T. A. (2013). Sorption of pollutants by porous carbon, carbon nanotubes and fullerene-an overview, Environ. Sci. Pollut. Res. 20 (5): 2828–2843.

Habib, N. R., Taddesse, A. M., and Temesgen, A., (2018). Synthesis, Characterization and Photocatalytic Activity of $Mn_2O_3/Al_2O_3/Fe_2O_3$ Nanocomposite for Degradation of Malachite Green. *Bull. Chem. Soc. Ethiop.*, 32(1), 101 – 109.

Ibrahim, M. A. and Ibrahim, M. B. (2018). Adsorption of Alkali Blue, Metanil Yellow and Neutral Red dyes Using Copper (II) Oxide particles: Kinetic and Thermodynamic Studies. *ChemSearch Journal*, 9(2): 13 – 23.

Kebede, T.G.; Mengistie, A.A.; Dube, S.; Nkambule, T.T.I.; and Nindi, M.M. (2018). Study on Adsorption of Some Common Metal Ions Present in Industrial Effluents by Moringa Stenopetala Seed Powder. *J. Environ. Chem. Eng.* 6, 1378–1389.

Khan, S. A., Manchanda, A. and Khan, T. A. (2024). Adsorption of Coomassie Brilliant Blue on a Novel Eco-Friendly Nanogel from Simulated Water: Equilibrium, Kinetic, and Thermodynamic Studies, *Chemistry Select*, 9, e202304927.

Kumar, N., Pandey, A., Rosy and Sharma, Y. C. (2023). A review on sustainable mesoporous activated carbon as adsorbent for efficient removal of hazardous dyes from industrial wastewater, *J. Water Process Eng.*, 54, 104054.

Kumari H.J., P. Krishnamoorthy, T. Arumugam, S. Radhakrishnan, and Vasudevan, D. (2017). An efficient removal of crystal violet dye from waste water by adsorption onto TLAC/Chitosan composite: a novel low cost adsorbent, Int. J. Biol. Macromol. 96: 324–333.

Latifi S., Saoiabi S., Alanazi M. M., Boukra O., Krime A., El Hammari L., *et al*. (2025), Low-Cost Titania-Hydroxyapatite (TiHAp) nanocomposites were synthesized for removal of Methylene blue under Solar and UV irradiation, *Next Materials*, 8, 100859, https://doi.org/10.1016/j.nxmate.2025.100859

Liu, X. J., Li, M. F. and Singh, S. K., (2021). Manganese-modified lignin biochar as adsorbent for removal of methylene blue. *Journal of Materials Research and Technology*, 12:1434-1445.

Lv, L., He, J., Wei, M., Evans, D.G. and Duan, X. (2006). Uptake of chloride ion from aqueous solution by calcined layered double hydroxides: Equilibruim and Kinetic studies. *Water Resources*, 40, 735-743.

Ma, Y., Ruan, Y. Xing, Du, D.X., La, Pa. (2017). Fabricaton of amino functionalized magnetic expanded graphite nanohybrids for application in removal Of Ag (I) from aqueous solution. *Journal of Nanomaterials*, 1 – 11.

Manzoor, K., Batool, M., Naz, F., Nazar, M. F., Hameed B. H. and Zafar, M. N. (2024). A comprehensive review on application of plant-based bioadsorbents for Congo red removal, *Biomass Conversion and Biorefinery*, 14, 4511–4537.

Marwani, H. M., Rahman M. M., Khan, S. B., Asiri, A. M., Alamry, K. A., Rub, M. A. and Chani, M. T. A. (2014). Selective detection of gold (III) ions based on codoped MnO_2–SnO_2 nanocubes prepared by solution method. *Materials Research Bulletin*, 51, 287–294

Moosavi, S., Lai, C. W., Gan, S., Zamiri, G., Pivehzhani, O. A. and Johan, M. R. (2020). Application of efficient magnetic particles and activated carbon for dye removal from wastewater, *ACS Omega*, 5, 20684–20697.

Moufi, H. F., Ansari, R. and Osovar, F. (2016). AgO/Sawdust Nanocomposite as an Efficient Adsorbent for removal of hexavalent Chromium Ions from Aqueous solutions. *Journal of Material and environment science.* 7(6), 2051-2068

Mousa, S.A., Abdallah, H., Ebnalwaled, A.A. *et al.* (2026). Highly efficient photocatalytic membrane based on green prepared SnO_2/PVC for industrial wastewater treatment. Appl. Phys. A 132, 243, https://doi.org/10.1007/s00339-026-09366-9

Muniyappa M., Rani Marilingaiah N., Rangappa D., Shetty M. (2026). SnO_2-coated stainless-steel electrodes: A promising approach for electrochemical oxidation in wastewater treatment, *Journal of Water and Environmental Nanotechnology*, 11 (1), 45-55,

Najafi, M., Bastami, T. R., Binesh, N., Ayati, A, and Emamverdi, S. (2022). Sono-sorption versus adsorption for the removal of congo red from aqueous solution using NiFeLDH/Au nanocomposite: Kinetics, thermodynamics, isotherm studies, and optimization of process parameters. *Journal of Industrial and Engineering Chemistry*, 116, 489–503.

Nangia, S., Katyal, D. and Warkar, S. G. (2023). Thermodynamics, kinetics and isotherm studies on the removal of anionic azo-dye (Congo red) using synthesized chitosan/Moringa oleifera gum hydrogel composites, *Sep. Sci. Technol.*, 58,13–28.

Nethaji S., Sivasamy A. And Mandal A. B. (2013). Adsorption Isotherms, Kinetics and Mechanism for the Adsorption of Cationic and Anionic Dyes onto carbonaceous particles prepared from Juglans Regia Shell Biomass, *International Journal of Environmental Science and Technology*, 10, 231–242

Rguiti M.M., Baddouh A., Elmouaden K., Bazzi Lh., Hilali M., Bazzi L. (2018), Electrochemical oxidation of olive mill waste waters on Tin Oxide Electrode, *J. Mater. Environ. Sci.* 9 (2), 551-558. https://doi.org/10.26872/jmes.2018.9.2.60

Salmani, M. H., Abedi, M., Mozaffari, S. A. and Sadeghian, H. A. (2017). Modification of pomegranate waste with iron ions a green composite for removal of Pb from aqueous solution: equilibrium, thermodynamic and kinetic studies. *AMB Express*. (2017)7, 225

Senapati, S., Giri, J., Mallick, L., Biswal, P., Behera, D., Rath, P. and Panda, A. K. (2025). Ultra-fast adsorption of the industrial cationic dye pollutant using nitric acid-activated rice straw biochar: insights into adsorption mechanisms. *Biomass conversion and Biorefinery*. 15: 18905-18923

Shaikh, W. A., Islam, R. U., Chakraborty, S. (2021). Stable silver nanoparticle doped mesoporous biochar-based nanocomposite for efficient removal of toxic dyes, *J. Environ. Chem. Eng.*, 9, 104982.

Singh, A., Verma, A. and Yadavz, B. C. (2022). MnO_2-SnO_2 Based Liquefied Petroleum Gas Sensing Device for Lowest Explosion Limit Gas Concentration. *ECS Sensors Plus*, 1: 025201

Tchinsa, A., Hossain, M. F., Wang T., Zhou Y. (2021) Removal of organic pollutants from aqueous solution using metal organic frameworks (MOFs)-based adsorbents: a review, *Chemosphere*, 284, 131393.

Tiwari A., Sandhwar V., Saxena S. *et al.* (2025). Advancements in SnO_2-based nanomaterials for efficient dye removal from wastewater. *Discov Sustain* 6, 636, https://doi.org/10.1007/s43621-025-01524-y

Wen, M., Li, G., Liu, H., Chen, J., An, T. and Yamashita, H. (2019). Metal-organic framework-based nanomaterials for adsorption and photocatalytic degradation of gaseous pollutants: recent progress and challenges, *Environ. Sci. Nano*, 6, 1006–1025.

Yaseen M., Humayun M., Khan A., Idrees M., Shah N., Bibi S. (2022). Photo-Assisted Removal of Rhodamine B and Nile Blue Dyes from Water Using CuO–SiO_2 Composite, *Molecules*, 27(16), 5343.